Influence of different contents of Si and Cu on the solidification pathways of cast hypoeutectic Al-(5–9)Si-(1–4)Cu (wt.%) alloys

Article *in* International Journal of Materials Research (formerly Zeitschrift fuer Metallkunde) · September 2013

DOI: 10.3139/146.110940

CITATIONS
5

READS
248

4 authors:

Mile B Djurdjevic
Nemak Linz
66 PUBLICATIONS **1,066** CITATIONS
SEE PROFILE

Srecko Manasijevic
Lola Institute Ltd
47 PUBLICATIONS **290** CITATIONS
SEE PROFILE

Zoran D Odanović
Welding & Welded Structures (Serbian Welding Society quarterly journal)
53 PUBLICATIONS **393** CITATIONS
SEE PROFILE

Radomir Radiša
Lola Institut
31 PUBLICATIONS **249** CITATIONS
SEE PROFILE

Mile B. Djurdjevic[a], Srecko Manasijevic[b], Zoran Odanovic[c], Radomir Radisa[b]
[a] Nemak Europe, Linz, Österreich
[b] Lola Institute, Belgrade, Serbia
[c] IMS Institute, Belgrade, Serbia

Influence of different contents of Si and Cu on the solidification pathways of cast hypoeutectic Al-(5–9)Si-(1–4)Cu (wt.%) alloys

A comprehensive understanding of the solidification process is of paramount importance for the control and prediction of actual casting characteristics. The present work presents the potential of cooling curve analysis to characterize the solidification path of a cast hypoeutectic series of Al–Si–Cu alloys. The aim of this work was to examine how variation in chemical composition of Si (from 5–9 wt.%) and Cu (from 1–4 wt.%) may affect characteristic solidification temperatures, their corresponding solid fraction, and thermal freezing ranges of the investigated alloys. All solidification parameters that have been calculated using cooling curve analysis show good correlation with the corresponding parameters calculated using commercial Pandat software. These parameters, either collected from the cooling curve analysis or calculated using Pandat software, can be easily incorporated into existing simulation software packages in order to improve their accuracy. In addition, cooling curve analysis can be used to estimate the effect of cooling rate on the above mentioned solidification parameters and used as additional input data for simulation.

Keywords: Aluminium alloys; Thermal analysis; Cooling curve analysis; Solid fraction analysis; Thermal freezing range

Nomenclature

FD	First Derivative
DCT	Dendrite Coherency Temperature
DCP	Dendrite Coherency Point
NTA	Newtonian thermal analysis
TFR	Thermal freezing range
T_{DCT}	Dendrite Coherency Temperature
T_c	Temperature at the center
T_w	Temperature at a nearby inner wall
T_{sol}	Solidus temperature
T_{liq}	Liquidus temperature
T_E^{Al-Si}	Al–Si eutectic temperature
$T_E^{Al-Si-Cu}$	Al–Si–Cu eutectic temperature
$f_{S95.0}$	Solid fraction value at f.e., 95.0 %
$f_{S95.0}$	Solid fraction value at f.e., 99.0 %
$f_{S99.5}$	Solid fraction value at f.e., 99.5 %
f_{DSP}	Solid fraction value at T_{DCT}
f_{NUC}^{Al-Si}	Solid fraction value at T_{NUC}^{Al-Si}
$f_{NUC}^{Al-Si-Cu}$	Solid fraction value at $T_{NUC}^{Al-Si-Cu}$

1. Introduction

The Al–Si–Cu alloys are widely used in the automotive industry due to their good casting characteristics and mechanical properties [1]. These alloys are characterized by the presence of two Al–Si and Al–Si–Cu eutectics, which are primarily responsible for defining the microstructure and mechanical properties of these alloys [1–4]. Comprehensive understanding of the solidification paths of these alloys is of paramount importance for metallurgical engineers. This knowledge enables the process, quality and simulation engineers as well as designers to ensure that the casting will achieve the desired properties for its intended application after corresponding melting, liquid metal processing, mould filling and heat treatment procedure. In order to ensure that cast components have good mechanical properties their as-cast microstructures must be closely monitored [2, 5].

Major alloying elements: Si, Cu and Mg are primarily responsible for defining the microstructure and mechanical properties of aluminium alloys [5]. The silicon is added to improve castability and fluidity, as well as to reduce shrinkage and to give superior mechanical and physical properties (the more Si an Al–Si–Cu alloy contains, the lower is the thermal expansion coefficient). Cu is the second major alloying element in these alloys. It has great impact on the strength and hardness of Al–Si–Cu alloys in as-cast and heat treated conditions. In additions, Cu reduces the corrosion resistance of aluminium alloys and in certain alloys increases stress corrosion susceptibility. The Mg role is also to improve the strength and hardness of Al–Si–Cu alloys in both as-cast and heat treated conditions. In order to ensure that cast components have good mechanical properties their as-cast microstructures must be closely monitored. Thermal analysis has such capabilities and has been used for many years in aluminium casting plants as a quality control tool [1, 6–10].

The thermal analysis (cooling curve) method is useful for commercial applications for a number of reasons: it is simple, inexpensive and provides consistent results. This technique is a good choice for drawing fundamental relation-

ships between cooling curve characteristics, alloy composition and melt treatment. Beside characteristic solidification temperatures, thermal analysis is often used to calculate solid fraction distribution between liquidus and solidus temperatures [11, 12].

The aim of this work is to examine how variation in chemical composition of Al-(5–9)Si-(1–4)Cu (wt.%) alloy may affect its characteristic solidification temperatures, solid fraction, and thermal freezing range. In order to accomplish this several experimental tests were carried out by applying the thermal analysis technique. All obtained data (characteristic solidification temperatures, solid fraction and other) could be incorporated in the current database in order to improve the accuracy of the existing simulation software programs.

The solidification pathways of Al–Si–Cu series alloys and formation of intermetallic and Cu enriched phases can be described according to many authors [1–4] as follows:

1. A primary α-aluminium dendritic network forms between 582–627 °C. The exact temperature depends mainly on the amount of Si and Cu and other alloying elements in the alloy. This leads to an increase in the concentration of alloying elements (Si, Cu, Mg…) in the remaining liquid.
2. Between 570–560 °C (the T_E^{Al-Si}) the eutectic mixture of Si and α-aluminium forms, leading to a further localized increase in the Cu content as well as increase in concentrations of other alloying elements that have been remained in residual liquid. Various contents of Cu, Mg, Zn and other alloying elements have significant impact on T_E^{Al-Si} while varying contents of Si does not change this temperature considerably. Additions of modifiers such as Sr or Na depress this temperature significantly.
3. In the temperature range 550–540 °C, the Mg_2Si and $Al_8Mg_3FeSi_6$ phases begin to precipitate.
4. At approximately 530 °C, the "massive" or "blocky" Al_2Cu phase (containing approximately 40 wt.% Cu) forms together with β-Al_5FeSi platelets.
5. Low 515 °C, a fine Al–Al_2Cu eutectic phase forms (containing approximately 24 wt.% Cu). If the melt contains more than 0.5 wt.% Mg, an ultra-fine $Al_5Mg_8 \cdot Cu_2Si_6$ eutectic phase also forms at this temperature. This phase grows from either of the two previously mentioned Al_2Cu phases.
6. The end of solidification (solidus temperature) is achieved in the range 505–477 °C. The presence of so called low melting point elements (Pb, Sn, Bi, Cd...) into Al–Si–Cu alloys will significantly extend the solidification ranges of these alloys depressing their corresponding solidus temperatures to lower values.

In the aluminium casting industry, the application of thermal analysis to study the development of the test sample structure was reported in early publications by Crossley [5] and Cibula [13]. In the late 1980s, this process control technology started to be used regularly in aluminium foundries [14]. The thermal analysis test samples can be taken either by submerging a cylindrical (graphite ceramic or steel) cup into the melt or pouring the melt by ladle into the test cup. One or two K-type thermocouples are placed into the melt and measure the temperature during solidification of the test sample. The outputs from the thermocouples are connected to a PC via data logger, where temperature/time data are recorded and later processed in various ways.

The solidification process of a metal or alloy is accompanied by the evolution of heat of various phases that form during the solidification. Recorded temperature–time data can yield quantitative information about the alloy solidification process. Such a plot is called a cooling curve and the general name given to the technique is thermal analysis. Major and minor metallurgical reactions (that are thermodynamically strong enough in terms of latent heat evolution) are manifested on the cooling curve by inflection points and slope change [1, 3, 6, 15, 16].

During the non-equilibrium solidification of the test samples, some thermally weak events cannot easily be detected on the cooling curve alone. Therefore, first and higher order derivatives plotted versus time or even temperature are utilized [1, 14]. The first derivative physically represents the rate of cooling (solidification) of the test sample. The second derivative represents the acceleration of the cooling rate during solidification. At present most European aluminium foundries regularly use thermal analysis to control the quality of the aluminium melt.

2. Experimental procedure

Twenty different Al–Si–Cu alloys with the chemical compositions as presented in Table 1 were produced. The content of the alloying elements varied between: 4.85–8.95 wt.% Si, 0.96–4.38 wt.% Cu, to ensure separation of the dominant phase in each of the tests. Their chemical compositions were determined using optical emission spectroscopy (OES).

The alloys were melted in an electric resistance furnace under protective nitrogen gas atmosphere to prevent hydrogen and oxygen contamination. A graphite crucible capacity of 10 kg was used throughout all the experiments. Commercially pure Si and Cu and Al-5Si (wt.%) master alloy were used as input materials to produce all investigated alloys. Unfortunately, some unwanted alloying elements from master alloy (Al-5Si (wt.%)) were detected in the test alloys (Table 1). Among them Mg and Sr are two elements that have significant impact on the solidification path of investigated alloys. No grain refining and modifier agents were added to the melt.

Samples with masses of approximately 300 g were poured into stainless steel cups. Two K-type thermocouples were inserted into the melt and temperatures between 750–400 °C were recorded. The data for thermal analysis was collected using a high-speed National Instruments data acquisition system linked to a personal computer. The sampling rate was 10 data per second. The cooling conditions were kept constant during all experiments and were approximately 6 K min^{-1}. The cooling rate was calculated as the ratio of the temperature difference between liquidus and solidus temperature to the total solidification time between these two temperatures. Each thermal analysis trial was repeated two times consequently, a total of 40 cooling curves were gathered.

3. Results and discussion

The results of cooling curve analysis are summarized in Table 2. All characteristic solidification temperatures were determined using either cooling curves or their correspond-

ing first derivatives. First derivative curves were plotted either as a function of time or temperature.

The dendrite coherency temperatures (DCT) were determined using the Bäckerud two thermocouples method [1]. In this method one thermocouple is located at the centre (T_c) of a test crucible, and the other at a nearby inner wall (T_w). The dendrite coherency point (DCP) is determined by identifying the local minimum on the ΔT versus time curve ($\Delta T = T_w - T_c$) and its projection on the T_c cooling curve and the reading of the corresponding temperature [1].

The reasoning that DCP occurs at this minimum ΔT versus time curve is based on the fact that the heat removal from the solid is faster than from the liquid phase. This is due to the significantly higher thermal conductivity of the

Table 1. Actual chemical composition of Al–Si–Cu test alloys, (wt.%).

Alloys	Chemical composition (wt.%)									
	Si	Cu	Mg	Ni	Fe	Mn	Zn	Ti	Sr	Al
$L_{5/1}$	4.85	1.03	0.14	0.008	0.09	0.01	0.01	0.058	0.0009	balance
$L_{5/2}$	5.01	2.06	0.26	0.007	0.10	0.01	0.01	0.062	0.0012	
$L_{5/3}$	4.97	2.98	0.21	0.009	0.07	0.01	0.01	0.058	0.0035	
$L_{5/4}$	4.89	3.85	0.16	0.009	0.09	0.01	0.01	0.090	0.0029	
$L_{6/1}$	5.90	1.07	0.14	0.008	0.07	0.01	0.01	0.063	0.0027	
$L_{6/2}$	5.90	1.83	0.15	0.009	0.11	0.01	0.01	0.062	0.0042	
$L_{6/3}$	5.82	3.03	0.15	0.008	0.06	0.01	0.01	0.059	0.0014	
$L_{6/4}$	5.78	3.96	0.13	0.007	0.07	0.01	0.01	0.075	0.0034	
$L_{7/1}$	7.13	0.96	0.28	0.007	0.12	0.01	0.01	0.056	0.0041	
$L_{7/2}$	7.05	1.98	0.28	0.009	0.13	0.01	0.01	0.079	0.0037	
$L_{7/3}$	6.95	3.05	0.26	0.007	0.14	0.01	0.01	0.081	0.0031	
$L_{7/4}$	6.75	4.38	0.29	0.008	0.12	0.01	0.01	0.091	0.0042	
$L_{8/1}$	8.03	1.09	0.28	0.008	0.14	0.01	0.01	0.093	0.0063	
$L_{8/2}$	8.14	1.93	0.27	0.009	0.12	0.01	0.01	0.084	0.0028	
$L_{8/3}$	8.03	2.96	0.29	0.007	0.14	0.01	0.01	0.096	0.0029	
$L_{8/4}$	7.84	4.30	0.30	0.009	0.14	0.01	0.01	0.090	0.0029	
$L_{9/1}$	8.92	1.05	0.31	0.009	0.12	0.01	0.01	0.062	0.0014	
$L_{9/2}$	8.95	2.04	0.31	0.007	0.12	0.01	0.01	0.081	0.0017	
$L_{9/3}$	8.91	3.11	0.29	0.007	0.15	0.01	0.01	0.073	0.0022	
$L_{9/4}$	8.85	4.38	0.27	0.008	0.14	0.01	0.01	0.056	0.0034	

Table 2. Characteristic solidification temperatures of Al–Si–Cu alloys determined using cooling curve analysis, (T, °C).

			Silicon (wt.%)				
			5	6	7	8	9
Copper (wt.%)	1	T_{liq}	626.6	622.4	613.3	600.7	597.3
		T_{DCP}	625.4	616.1	611.1	598.7	593.5
		T_E^{Al-Si}	572.4	573.7	570.3	575.0	568.5
		$T_E^{Al-Si-Cu}$	543.6	518.7	526.2	517.4	526.3
		T_{sol}	480.2	501.7	482.3	501.8	483.1
	2	T_{liq}	622.8	618.9	610.3	601.7	589.9
		T_{DCP}	621.0	615.0	606.1	597.9	587.1
		T_E^{Al-Si}	567.2	570.5	569.0	572.2	564.6
		$T_E^{Al-Si-Cu}$	534.5	518.3	508.5	517.2	506.5
		T_{sol}	477.9	502.2	480.4	499.4	480.1
	3	T_{liq}	620.0	614.8	607.4	600.5	587.3
		T_{DCP}	617.9	611.7	602.6	591.0	583.5
		T_E^{Al-Si}	560.5	569.3	562.2	569.3	562.7
		$T_E^{Al-Si-Cu}$	524.0	522.0	507.4	517.7	505.4
		T_{sol}	478.6	502.7	482.1	494.5	480.5
	4	T_{liq}	618.3	610.3	604.6	596.8	583.5
		T_{DCP}	616.2	608.3	600.2	587.8	581.4
		T_E^{Al-Si}	552.2	566.9	558.9	565.9	562.9
		$T_E^{Al-Si-Cu}$	512.0	522.9	509.6	516.3	508.1
		T_{sol}	480.6	501.8	481.9	495.7	480.5

solid dendrites (forming the network) in comparison to the surrounding liquid metal.

From Table 2 it is obvious that increasing the Si and Cu contents significantly decreases all characteristic solidification temperatures.

3.1. Cooling curve analysis–Liquidus temperature

The liquidus temperature (T_{liq}) specifies the maximum temperature at which the crystal can coexist with the melt in thermodynamic equilibrium. Above T_{liq} no crystals exist and the melt is liquid and homogeneous. This temperature is very important in the casting industry because it defines the preheating temperature (difference between the liquidus and pouring temperatures) and initial or pouring temperature of the melt.

Tables 2 and 3 show characteristic solidification temperatures of the Al-(5–9)Si-(1–4)Cu (wt.%) series of alloys that were determined either using cooling curve analysis (Table 2) or Pandat [17] software (Table 3). In order to eliminate the impact of the cooling rate on the depression of characteristic solidification temperatures during all experiments the cooling rate was kept constant ($\sim$ 6 K min^{-1}). From both Tables 2 and 3 it is clear that any increase in the content of Si and Cu depresses the characteristic solidification temperatures. According to the results obtained using cooling curve analysis increasing the Si content for one weight percent depress the T_{liq} by 6.5 °C (5.7 °C/1 wt.% Si using Pandat calculation) with constant Cu content. The obtained results are in fair agreement with the binary Al–Si phase diagram, where increase of Si content up to eutectic concentration ($\sim$12.3 wt.%) decreases the T_{liq} by 83 °C (the temperature drops almost linearly from 660–577 °C) which is approximately a decrease of 6.7 °C per 1 wt.% Si.

Considering the impact of varying Cu content on the depression of T_{liq} similar results have been obtained either using Pandat calculation (Scheil mode) or cooling curve analysis. One weight percent of Cu with constant Si content decreases the T_{liq} by approximately 2.4 °C which is a lower value than expected according to the equilibrium binary Al–Cu phase diagram (3.3 °C/1 wt.% Cu). One of the reason for this difference can be found in the fact that a limited range of Cu content has been analyzed (up to 4.38 wt.%) during experiments to calculate the impact of 1 wt.% Cu on depression of T_{liq}, in comparison to a significantly broader concentration range (up to 33 wt.%) taken from binary Al–Cu phase diagram.

3.2. Cooling curve analysis–Dendrite coherency temperature

During the solidification of any aluminium hypoeutectic alloy, a dendritic network of primary α-aluminium crystals will be developed. In the early stage of solidification dendritic crystals are separate and move freely in the melt. However, as the melt cools, the dendrite tips of the growing crystals begin to impinge upon one another until a coherent dendritic network is formed [18]. The temperature at which this occurs is called the dendrite coherency temperature (T_{DCT}) and is a very important feature of the solidification process [18–21]. This temperature marks the moment when the "mass" feeding changes to interdendritic feeding [1, 18–22]. Casting defects such as macrosegregation, shrinkage porosity and hot tearing begin to develop after the DCT [18–22].

The DCT is a physical phenomenon; however its direct detection is virtually impossible. There are two main approaches for detection of T_{DCT}: (i) Mechanical (or rheologi-

Table 3. Characteristic solidification temperatures of Al–Si–Cu alloys calculated using Pandat program and Scheil solidification model, (T, °C).

			Silicon (wt.%)				
			5	6	7	8	9
Copper (wt.%)	1	T_{liq}	626.9	619.9	611.4	605.8	598.7
		T_{DCP}	NA	NA	NA	NA	NA
		T_E^{Al-Si}	570.0	571.9	571.8	573.7	572.4
		$T_E^{Al-Si-Cu}$	515.9	515.5	533.7	522.5	534.2
		T_{sol}	509.9	509.9	509.9	509.9	509.9
	2	T_{liq}	622.1	617.3	608.5	602.1	594.9
		T_{DCP}	NA	NA	NA	NA	NA
		T_E^{Al-Si}	566.5	569.4	569.2	571.9	570.4
		$T_E^{Al-Si-Cu}$	514.1	513.6	518.7	523.0	521.3
		T_{sol}	509.9	509.9	509.9	509.9	509.9
	3	T_{liq}	619.7	614.1	605.6	599.3	591.4
		T_{DCP}	NA	NA	NA	NA	NA
		T_E^{Al-Si}	564.3	566.3	566.6	569.5	568.3
		$T_E^{Al-Si-Cu}$	515.0	517.2	512.9	523.2	511.6
		T_{sol}	509.9	509.9	509.9	509.9	509.9
	4	T_{liq}	617.7	611.4	602.4	595.9	587.3
		T_{DCP}	NA	NA	NA	NA	NA
		T_E^{Al-Si}	561.8	563.9	563.2	566.6	566.1
		$T_E^{Al-Si-Cu}$	518.6	519.6	515.2	523.3	515.7
		T_{sol}	509.9	509.9	509.9	509.9	509.9

Table 4. Characteristic fraction solid values of Al–Si–Cu alloys determined using cooling curve analysis.

			Silicon (wt.%)				
			5	6	7	8	9
Copper (wt.%)	1	f_{DSP}	8.61	16.17	7.70	13.85	6.05
		f_{NUC}^{Al-Si}	62.28	51.08	43.33	33.64	27.65
		$f_{NUC}^{Al-Si-Cu}$	95.47	99.08	96.48	98.40	96.67
	2	f_{DSP}	8.32	3.10	6.58	14.01	8.18
		f_{NUC}^{Al-Si}	60.00	51.82	41.21	34.67	26.22
		$f_{NUC}^{Al-Si-Cu}$	93.41	97.75	96.11	96.92	95.31
	3	f_{DSP}	7.90	3.34	6.01	15.12	7.71
		f_{NUC}^{Al-Si}	59.36	51.32	40.79	31.71	23.74
		$f_{NUC}^{Al-Si-Cu}$	92.58	95.66	93.08	94.35	92.85
	4	f_{DSP}	7.54	3.24	5.92	13.95	6.90
		f_{NUC}^{Al-Si}	58.71	48.94	40.26	30.67	21.45
		$f_{NUC}^{Al-Si-Cu}$	91.78	92.76	90.84	91.21	91.55

cal) methods [22] and (ii) Thermal detection methods [1, 18]. In this work the DCTs has been determined for each set of experiments using the traditional two thermocouples technique developed by Bäckerud [1]. The solidification conditions, chemical composition of the alloy and addition of grain refiners are major factors that have significant impact on the dendrite coherency temperature. Independent from applied measured techniques, it has been verified that faster cooling rate and increase in solute concentration postpone the coherency point to lower temperatures [1, 18–21].

The influence of Si and Cu on the T_{DCT} is presented in Fig. 1. The higher Si and Cu contents progressively reduce the T_{DCT}. The impact of Si is more significant (decrease in T_{DCT} of $\sim$6.75 °C per 1 wt.% Si) than that of Cu (decreasing T_{DCT} of $\sim$2.55 °C per 1 wt.% Cu). The obtained results are in agreement with the available literature data [1, 18, 21]. These results are not unexpected. It is well known that the sizes of the dendrites are influenced by the levels of alloying elements present in the melt (of course the main influence is the solidification rate). During the primary solidification of the aluminium alloys the alloying elements are not evenly distributed between solid and liquid phases. Excess amount of solute displaced away from the solidification interface into the melt results in an increase in volume of solute located between already formed dendrite arms. This super saturation (or related constitutional undercooling) represents the driving force for the growth of the dendrites. The space between α-aluminium dendrite arms must increase to accommodate an increasing amount of solute elements. Clearly then a higher concentration of alloying elements will reduce the growth of dendrites and postpone their contact (coherency) to lower temperature. It is also expected that the elements having a higher solubility in the aluminium melt are less effective in reducing the size of the secondary dendrite arm spacing (*SDAS*). Therefore, the effect of the same content of Cu (maximum solubility of Cu in Al is 5.7 wt.%) is significantly less than that of the same amount of Si (maximum solubility of Si in Al is 1.6 wt.% Si).

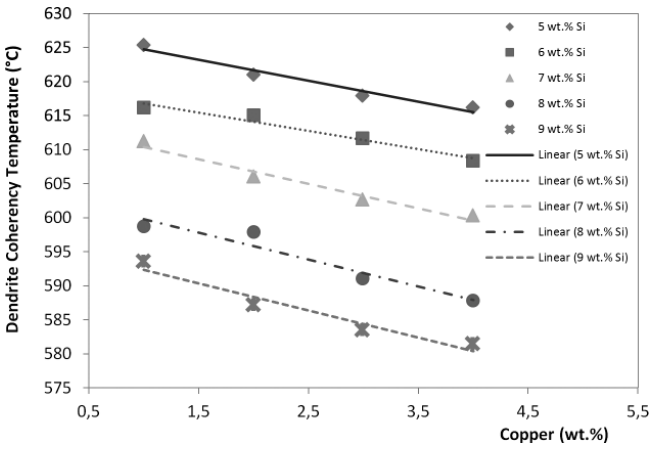

Fig. 1. Impact of various Si and Cu contents on the T_{DCT}.

3.3. Cooling curve analysis–Al–Si eutectic temperature

In order to control the quality of aluminium melts (e. g., level of modification) or for simulation purpose (to know the amount of solid fraction at the Al–Si eutectic temperature (T_E^{Al-Si}) it is necessary to know the T_E^{Al-Si} of the aluminium alloys with the highest possible degree of accuracy. Tables 2 and 3 reveal that the additions of Si and Cu in the investigated alloys change this temperature considerably. Increase in the Cu content from 1–4 wt.% with constant Si content, dropped this temperature by $\sim$10.6 °C (by Pandat calculation this decrease was approximately 7.6 °C). Increase in the Si content from 5–9 wt.% with constant Cu content lowered this temperature by $\sim$9 °C according to thermal analysis measurements (depression by Pandat calculation was significantly lower $\sim$5 °C). The main reason for the stronger impact of Si and Cu on the values of T_E^{Al-Si} determined using cooling curve analysis is the fact that all the investigated alloys have considerable amounts of residual Sr (from 9–63 ppm Sr). It is well known that Sr has significant impact on the depression of T_E^{Al-Si}. Recent investigation has shown that even a relatively small increase in the amount of added Sr (e. g. 38 ppm) depressed the T_E^{Al-Si} for approximately 6.5 °C [3]. Unfortunately, presently market-available software packages (Pandat, JMatPro, FactSage, …) are not capable of taking into consideration the impact of small amounts of Sr (in ppm range) on the characteristic

Table 5. Characteristic fraction solid values of Al–Si–Cu alloys calculated using Pandat program and Scheil solidification mode.

			Silicon (wt.%)				
			5	6	7	8	9
Copper (wt.%)	1	f_{DSP}	NA	NA	NA	NA	NA
		f_{NUC}^{Al-Si}	65.07	56.16	46.92	38.28	31.29
		$f_{NUC}^{Al-Si-Cu}$	98.41	98.24	97.37	98.46	96.35
	2	f_{DSP}	NA	NA	NA	NA	NA
		f_{NUC}^{Al-Si}	61.96	54.65	45.36	35.89	29.65
		$f_{NUC}^{Al-Si-Cu}$	96.28	96.64	95.58	96.69	95.55
	3	f_{DSP}	NA	NA	NA	NA	NA
		f_{NUC}^{Al-Si}	60.35	53.61	43.57	34.44	26.40
		$f_{NUC}^{Al-Si-Cu}$	94.00	94.05	93.88	94.37	94.23
	4	f_{DSP}	NA	NA	NA	NA	NA
		f_{NUC}^{Al-Si}	59.26	51.99	42.60	32.64	24.78
		$f_{NUC}^{Al-Si-Cu}$	92.30	92.32	91.15	91.66	91.49

solidification temperatures of Al–Si–Cu alloys. Therefore, there is this difference in the depression of the T_E^{Al-Si} measured using cooling curve analysis and calculated by means of the Pandat Scheil solidification method. According to Heusler and Schneider [23] Mg has strong influence on T_E^{Al-Si}. Based on their own investigations it has been found that increasing the Mg content in Al-11Si (wt.%) alloy (without Sr) up to 1 wt.% drops the T_E^{Al-Si} by 11 °C. Applying the equation developed by Heusler and Schneider [23] it has been calculated that lower Mg content in the investigated alloy (0.14 wt.% Mg) depressed T_E^{Al-Si} by 0.766 °C while the highest content of Mg (0.31 wt.% Mg) decreased this temperature by almost 2 °C. The introduction of Cu into Al–Si alloys results in a lowering of the T_E^{Al-Si}. It has been shown in the literature [1] that introduction of Cu into Al-9Si (wt.%) alloys results in a lowering of the eutectic temperature of 8 °C (T_E^{Al-Si} of Al-9Si (wt.%) alloy without Cu was 576.5 °C and 568.5 °C with 3.5 wt.% Cu). This result is in excellent agreement with the results presented in Table 2, obtained using cooling curve analysis.

3.4. Cooling curve analysis–Al–Si–Cu eutectic temperature

From Tables 2 and 3 it is clear that increasing the Si (from 5–9 wt.%) and Cu (from 1–4 wt.%) contents significantly changes the Al–Si–Cu eutectic temperatures ($T_E^{Al-Si-Cu}$). These results indicate that Cu enriched phase(s) precipitate at different temperatures depending on the amount of Si and mainly Cu present in the particular alloys. According to results presented in Table 2, when the Cu content increased from 1–4 wt.% the $T_E^{Al-Si-Cu}$ reduced (except for Al-6Si-(1–4)Cu (wt.%) alloys, where this temperature slightly increased). This impact is due to segregation of Cu during precipitation of other constituents that solidified before Cu-rich phase(s). According to Pandat calculation, the contents of Cu just before the start of Cu-rich eutectic formation (in residual liquid) were between 4.35 and 27.35 wt.% for Al-5Si-1Cu (wt.%) and Al-5Si-4Cu (wt.%) alloys respectively. The addition of the Cu into Al-(5–9) Si-(1–4)Cu (wt.%) alloys also results in a lowering of the $T_E^{Al-Si-Cu}$. The data presented in Table 2 show that $T_E^{Al-Si-Cu}$ is decreased by between 20 °C (Al-5Si-(1–4)Cu (wt.%)) and 5 °C (Al-9Si-(1–4)Cu (wt.%)) due to increased Cu content.

The number and shape of the peaks visible in the Cu-enriched region of the first derivative curves plotted versus temperature, show a strong relationship with the amount of Cu present in the alloy (for more details see Fig. 2). The precipitation temperature of the Cu-enriched phases decreases when Cu content increases from 1 to 4 wt.% Cu. The Cu-enriched phase represented by the first peak on the cooling curve in Fig. 2 (6 wt.% Si, 1 wt.% Cu alloy) began to solidify at 518.7 °C and the Cu-enriched phase represented by the second peak appeared at 503.9 °C. In the alloy with 6 wt.% Si, 2 wt.% Cu alloy two peaks appeared at temperatures of 518.3 °C and 506.7 °C respectively. Increasing the amount of Cu to 3 wt.% (6 wt.% Si) further changes the shape of the Cu-enriched phase peaks (Fig. 2). Now two separated peaks are recognized and their solidification temperatures are also altered. The Cu-enriched phase represented by the first peak for the Al-6Si-3Cu (wt.%) alloy begins to solidify at 522.0 °C, while second peak appears at 508.1 °C. In the last investigated alloy (Al-6Si-4Cu (wt.%) first Cu-rich peak appears at 522.9 °C while the second peak corresponds to 509.8 °C. Similar impact of the Cu contents has been observed in all other investigated alloys [3]. According to Samuel [24] the Cu phases solidify in three dis-

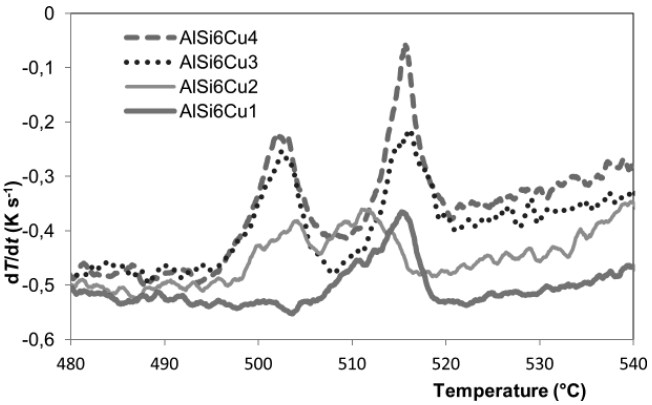

Fig. 2. First derivative of the Al-6Si-(1–4)Cu (wt.%) cooling curves related to Cu enriched region.

tinct forms: two eutectics ($Al-Al_2Cu$ eutectic and ultra-fine $Al_5Mg_8Cu_2Si_6$ copper eutectic) and blocky phase (Al_2Cu). Samuel [24] as well as the other researchers [25, 26] found that the increase in the Sr content increases the proportion of blocky-Al_2Cu and ultra-fine $Al_5Mg_8Cu_2Si_6$ copper phases versus $Al-Al_2Cu$ eutectic Cu. All first derivative curves from our experiments have one or two visible Cu-rich eutectic peaks. This means that some of the Cu phases detected by Samuel and other researchers are mostly convoluted (not visible on the first derivative curves) due to weak latent heats released during precipitation of these phases. Increasing the content of Mg (some authors [4] suggested greater than 0.5 wt.% Mg), results in the precipitation of $Al_5Mg_8Cu_2Si_6$ copper eutectic (occurring as branched crystals or fine eutectic strings growing out from Al_2Cu blocky or $Al-Al_2Cu$ eutectic types during the final stage of solidification). The addition of strontium leads to an increase of the Al_2Cu blocky type [4]. Some other elements (Pb, Sn, Bi, Ca, P, Sb and P) present in Al–Si–Cu alloys in small amounts (ppm range) can also have significant impact on the T_E^{Al-Si} and $T_E^{Al-Si-Cu}$ and precipitation morphology of Cu-rich phases. Fortunately the alloys investigated in this paper had either very low amounts of such elements (lower that 5 ppm) or they were not even detected in the investigated alloys. Therefore, the impact of these elements on characteristic solidification temperatures and solidified copper morphology has not been considered in this paper. In the literature there are several papers that extensively studied the impact of major and minor alloying elements on the depression of characteristic solidification temperature of aluminium alloys as well as their impact on solidified morphologies [4, 7–9, 26–29].

3.5. Cooling curve analysis–Solidus temperature

The solidus temperature (T_{sol}) identifies the temperature at which the last portion of the liquid has transformed to solid. Below this temperature the given alloy is stable in the solid phase. The results presented in Tables 2 and 3 indicate that varying Si and Cu contents in the investigated alloys have the lowest impact on T_{sol}. According to Pandat results this temperature is constant (509.9 °C). The average T_{sol} determined using cooling curve analysis, for all investigated alloys, was ~488 °C significantly lower than that calculated using Pandat software.

As can be seen from Table 2, the T_{sol} for all investigated alloys show significant inconsistencies. The difference in T_{sol} is largely due to difficulties in defining when the last drop of the liquid solidified. Applying smoothing for all derivative curves also brings some inaccuracy to thermal analysis measurement. In addition some other electrical devices in the casting plant (e. g., induction furnace) could affect the accuracy of the collected results. More about various sources that could have impact on the inconsistency of thermal analysis measurement can be found at the MeltLab web page http://www.meltlab.com by Sparkman [25]. As a potential solution to this problem we propose applying the solid fraction versus temperature curve. The T_{sol} can be determined by cutting off the solid fraction value at e. g., 99.0 % ($f_{S99.0}$) and picking up its corresponding temperature as an exact solidus. This hypothesis will be tested in a forthcoming paper.

3.6. Solid fraction analysis

Besides characteristic solidification temperatures, the thermal analysis is often used to calculate solid fraction distribution between T_{liq} and T_{sol}. A critical requirement for the solid fraction calculation applying cooling curve analysis is determination of what is called a base line [1, 11, 12]. The base line is in principle the first derivative of the cooling curve measured by the thermocouple(s), inserted in the alloy test sample, assuming that the metal does not undergo any phase transformation during the solidification process. In other words the base line overlaps the first derivative of the cooling curve in single phase parts of the sample cooling process, for temperatures higher than T_{liq} and for temperatures lower than T_{sol}.

In the literature are two methods, Newtonian and Fourier analysis [11, 12], that have been successfully used to calculate solid fraction distribution using cooling curve analysis. In this work only Newtonian thermal analysis (NTA) has been applied to calculate the base line using cooling curve analysis. Solid fraction distribution between T_{liq} and T_{sol} was calculated using cooling curve analysis (NTA method) and Pandat software program (Scheil Mode) Tables 4 and 5 respectively.

Comparison of solid fraction values detected at T_E^{Al-Si} for all investigated Al-(5–9)Si-(1–4)Cu (wt.%) hypoeutectic alloys using thermal analysis and Pandat software are presented in Fig. 3. Both sets of results show the same tendency. By increased contents of Si and Cu in Al melts the fraction solid values at T_E^{Al-Si} decreased. Values calculated using Pandat software packages (open symbols) showing a trend to be a little bit higher than values determined using cooling curve analysis (filled symbols). From Fig. 3 it is obvious that the impact of Si content is more significant than that of Cu. The obtained values are very important for simulation engineers, who use these solid fraction values as a feeding criterion during simulation.

A similar approach can be applied for determining the area fraction of individual phases that precipitate during solidification of Al–Si–Cu alloys. It is evident from Fig. 4 that the area between path ($T_{NUC}^{Al-Si} - T_{sol}$) and the first derivative of the cooling curve (FD) should be proportional to the latent heat of solidification of the Cu enriched phases.

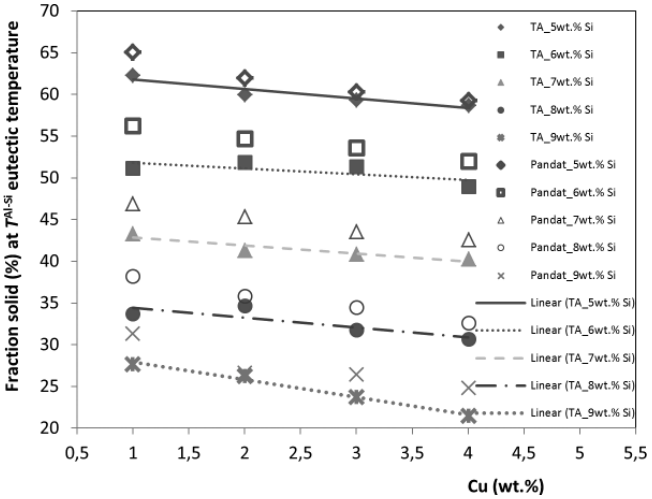

Fig. 3. Impact of Si and Cu content on the distribution of the solid fraction at T_E^{Al-Si}.

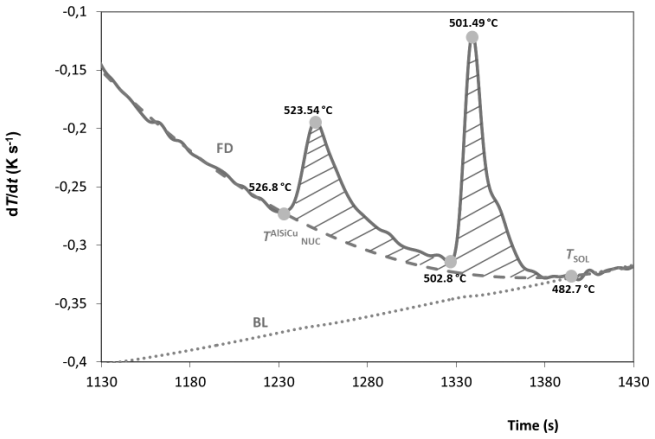

Fig. 4. The part of the first derivative curve related to Cu-rich phase.

Recently, it has been shown that the total area fraction of the Cu enriched phases determined using image analysis correlated very well with an integrated area (hatched area on Fig. 4.) of the Cu-enriched phases of Al–Si–Cu alloys [26].

3.7. Thermal freezing range

Another useful criterion that can be extracted from the calculated solid fraction curve is the non-equilibrium partial freezing range near termination of solidification that according to [30] has been abbreviated as the thermal freezing range (TFR). The TFR has a significant impact on the hot tearing formation. In general as the freezing range increases the hot tearing susceptibility also increases. The chemical composition is the main influencing factor on the freezing range. Unfortunately, a range in which this criterion has to be calculated has not yet been established.

In this paper a range between 95.0 % and 99.5 solid % fraction (TFR ($f_{S95} - f_{S99.5}$)) recently proposed by Pabel et al. [31, 32] has been used. In this work, the TFR was determined using fraction solid curves which have been calculated either using data from cooling curve analysis or Pandat data obtained applying the Scheil solidification method.

Tables 6 and 7 summarize TFRs that have been calculated using both above mentioned approaches. Analyzing results from Table 6 it could be concluded that increases of 1 wt.% in Cu decrease TFR by $\sim$8.2 °C, while the increases of 1 wt.% in Si reduces the TFR by $\sim$1.75 °C. From both Tables (6 and 7) it is evident that Cu contents have a larger impact on the hot tearing formation than Si contents. Experimental evaluation of the hot tearing tendency in aluminium alloys is very complex. Cooling curve analysis has the potential to quantify these criteria and should be used more often.

In this work only the cooling curve, its first derivative, ΔT curve and the calculated solid fraction curve have been used to determine various solidification parameters of the investigated alloys. According to some researchers [33, 34] this is not the end of cooling curve application. According to Sparkman [33] higher order derivatives offer the possibility of introducing thermal analysis to become much more than just a quick quality control tool. With the ability to actually measure the energy of individual phases, shrinkage and stress, many more characteristics of the aluminium

Table 6. Characteristic TFR ($f_{S95} - f_{S99.5}$) of Al–Si–Cu alloys determined using cooling curve analysis.

		Silicon (wt.%)				
		5	6	7	8	9
Copper (wt.%)	1	49.56	39.48	42.59	36.34	40.76
	2	34.10	38.80	25.07	23.40	11.50
	3	19.62	22.13	13.45	12.37	9.85
	4	9.62	14.38	4.75	9.43	7.02

Table 7. Characteristic TFR ($f_{S95} - f_{S99.5}$) values of Al–Si–Cu alloys calculated using Pandat program (Scheil solidification mode).

		Silicon (wt.%)				
		5	6	7	8	9
Copper (wt.%)	1	42.98	41.08	38.57	36.55	4.61
	2	18.63	21.25	12.57	19.38	16.56
	3	3.58	6.48	0.67	4.40	0.12
	4	5.53	7.28	0.27	3.04	0.02

alloys will be available through the measurements run on the foundry floor [33]. Applying new generation of data loggers, high speed computers, high precision thermocouples and good mathematical procedures many of the currently unidentified parameters from the cooling curves and their derivatives will be more easily detected and could potentially be used as input data for available simulation software packages.

4. Conclusions

A comprehensive understanding of the solidification process is of paramount importance for the control and prediction of actual casting characteristics. This work has shown that thermal analysis is a valuable tool widely used in aluminium foundry that can collect numerous parameters (characteristic solidification temperatures, solid fraction distribution, fraction of particular phases and TFR) beneficial for better understanding the solidification path of Al–Si–Cu alloys. In addition, the data collected using cooling curve analysis should be applied in existing simulation software in order to improve accuracy of simulation.

The interest in simulation applied in the aluminium casting industry has grown significantly in the last few decades. Three main reasons are responsible for that: (i) the necessity to improve productivity and quality of cast products (ii) to speed up the design process and (iii) to investigate the influence of different process parameters without the need for expensive experimental trials. The accuracy of casting simulation depends a great deal on the quality of the available physical and thermophysical material properties provided by the software's database. Available databases presently used by commercial simulation software packages for the casting industry usually come with material properties for only a few selected standard alloys. Certainly, the industrial interest is to be able to make simula-

tion and optimization based on more realistic databases in order to more reliably predict the quality of very complex cast parts. Thermal analysis has such an opportunity, and has to be used more often in providing simulation engineers with all necessary data for simulation in synergy with commercial software packages.

Final casting products contain different cross-section thicknesses that solidify under different cooling rates, which in turn affect the as-cast structure. In order to be able to simulate such intricate cast products it is necessary to have a deeper understanding of the effect of cooling rate on the solidification process. Thermal analysis is a useful tool to help estimate the effect of cooling rate on the resulting cast structure. The thermal analysis apparatus is capable of collecting the cooling curves for solidification under various cooling rates. For each cooling rate all above mentioned parameters can be measured/calculated and used as input data for simulation.

This work has been supported by the Ministry of Education, Science and Technological Development of the Republic of Serbia (Projects ON 172005 and TR 35023).

References

[1] L. Bäckerud, G. Chai, J. Tamminen: Solidification Characteristics of Aluminium Alloys, AFS/SKANALUMINIUM, Oslo, 2 (1986) 95.
[2] C.H. Caceres, M.B. Djurdjevic, T.J. Stockwell, H.J. Sokolowski: Scr. Mater.40 (1999) 631. DOI:10.1016/S1359-6462(98)00492-8
[3] M.B. Djurdjevic, T. Stockwell, J. Sokolowski: Int. J. Cast Met. Res. 12 (1999) 67.
[4] H.W. Doty, A.M. Samuel, F.H. Samuel: 100th AFS Casting Congress, Philadelphia, Pennsylvania, USA (1996) 1.
[5] P.B. Crossley, L.F. Mondolf: Modern Casting 49 (1966) 53.
[6] S. Argyropoulos, B. Glosset, J. Gruzleski H. Oger: AFS Transaction 27 (1983) 351.
[7] G.K. Sigworth: AFS Transaction 66 (1983) 7.
[8] L. Wang, S. Shivkumar: J. Mater. Sci. 30 (1995) 1584. DOI:10.1007/BF00375269
[9] M. Garat, G. Laslaz, S. Jacob, P. Meyer, P.H. Guerin, R. Adam: AFS Transaction 146 (1992) 821.
[10] D. Apelian, G.K. Sigworth, K.R. Wahler: AFS Transaction 161 (1984) 297.
[11] E. Fras, W. Kapturkiewicz, A. Burbielko, H.F. Lopez: AFS Transactions 101 (1993) 505.
[12] W.T. Kierkus, J.H. Sokolowski: AFS Transactions 66 (1999) 161.
[13] A. Cibula: J. Inst. Met. 80 (1952) 1.
[14] D. Sparkman, A. Kearney: AFS Transactions 113 (1994) 455.
[15] J.E. Gruzleski, B.M. Closset: Treatment of liquid aluminium-silicon alloys, AFS Inc., Des Plaines, IL, USA (1990) 25.
[16] N. Tenekedjiev, H. Mulazimoglu, B. Closset, J. Gruzleski: Microstructures and thermal analysis of strontium-treated aluminium-silicon alloys, AFS Inc., Des Plaines, IL, USA (1995) 40.
[17] http://www.computherm.com/pandat.html.
[18] L. Bäckerud, B. Chalmers: Trans. Metall. Soc. AIME, 245 (1969) 309.
[19] J. Tamminen: Chem. Comm., Stockholm University, Sweden, 2 (1988) 8.
[20] G. Chai: Chem. Comm., Stockholm University, Sweden, 1 (1994) 59.
[21] N. Veldman, A.K. Dahle, D.St. John, L. Arnberg: Metall. Mater. Trans. A32 (2001) 147. DOI:10.1007/s11661-001-0110-1
[22] H. Jiang, W.T. Kierkus, J.H. Sokolowski: AFS Transactions 68 (1999) 169.
[23] L. Heusler, W. Schneider: J. Light Met. 2 (2002) 17. DOI:10.1016/S1471-5317(02)00009-3
[24] F.H. Samuel: J. Mater. Sci. 33 (1998) 2283. DOI:10.1023/A:1004383203476
[25] D. Sparkman: Improving the Accuracy of Thermal Analysis, MeltLab Systems LLC, 2008.
[26] M.B. Djurdjevic, W. Kasprzak, C.A. Kierkus, W.T. Kierkus, J.H. Sokolowski: AFS Transactions 24 (2001) 1.
[27] M.B. Djurdjevic, D. Muche, B. Stauder, K. Eigenfeld: Prakt. Metallogr. 49 (2012) 356.
[28] M.B. Djurdjevic, Z. Odanovic, N. Talijan: JOM 63 (2011) 51. DOI:10.1007/s11837-011-0067-5
[29] H. Beumler, A. Hammerstad, B. Wieting and R. DasGupta: AFS Transactions 54 (1988) 1.
[30] D. Apelian, J.J.A. Cheng: AFS Transactions 94 (1986) 797.
[31] M.B. Djurdjevic, R. Schmid-Fetzer: Mater. Sci. Eng. A 417 (2006) 24. DOI:10.1016/j.msea.2005.08.227
[32] T. Pabel, S. Bozorgi, C. Kneissl, K. Haberl, P. Schumacher: Giesserei Praxis 12 (2010) 388.
[33] D.A. Sparkman: AFS Transactions 119 (2011) 1.
[34] R.C. Zamarripa, J.A. Ramos-Salas, J. Talamantes-Silva, S. Valtierra, R. Colas: Mater. Sci. Eng. A 38 (2007) 1875.

(Received November 28, 2012; accepted March 15, 2013)

Bibliography

DOI 10.3139/146.110940
Int. J. Mater. Res. (formerly Z. Metallkd.)
104 (2013) E; page 1 – 9

ISSN 1862-5282

Correspondence address

Srecko Manasijevic, Ph. D.
Kneza Viseslava 70a
11 000 Belgrade
Serbia
Tel.: +381 11 257 7604
E-mail: srecko.manasijevic@li.rs

You will find the article and additional material by entering the document number **MK110940** on our website at *www.ijmr.de*